Comparison between SWCNT Interconnects and Copper Interconnects for GSI and TSI Integrated Circuits

C. P. S. M. Nogueira, J. G. Guimarães

***Abstract*—**Carbon nanotubes are an extremely attractive option as interconnects for giga (GSI) and tera (TSI) scaled integrated circuits. They are promising candidates to replace copper interconnects. This paper presents a study of single-walled carbon nanotubes (SWCNTs) and copper as interconnects. The circuit model is presented and a comparison between isolated SWCNT and SWCNT bundle at different lengths is studied, analyzing their frequency, attenuation and delay time. For this purpose, the interconnects were simulated using the LTSpice software.

***Keywords*—**Carbon nanotubes, copper, interconnects, integrated circuits.

I. Introduction

THE miniaturization of integrated circuits is quite challenging in interconnect projects. New technologies are being studied to overcome copper interconnects limitations in circuits, such as electrical proprieties and electromigration reliability, especially in technology below 45 nm [1],[2]. The optical interconnects, radio frequency or wireless interconnects, and carbon nanotubes (CNT) interconnects are some of the candidates to replace copper interconnects [2]-[5]. Among the possibilities, the CNTs interconnects have great advantages for GSI and TSI integrated circuits [1]-[6]. They are considered efficient solutions to improve copper interconnection problems, such as delay, power dissipation and resistance to electromigration. According to the International Technology Roadmap for Semiconductors (ITRS) [7], the 22 nm technology node is the technology that should be used by the year 2016.

Camila P.S.M. Nogueira received the B.E. and the M.E. degree in electrical engineering from University of Brasília, Brasília, Brazil, in 2010 and 2012, respectively. Since 2012 she has been working for the Brazilian Government. Her research interests include interconnects, single-electron devices, neural networks and models.

Prof. Dr. J. G. Guimarães is with the Federal University of Santa Catarina, Campus Blumenau, Blumenau, Brazil (e-mail : janaina.guimaraes@ufsc.br)

The CNTs have led to considerable interest among scientists since its discovery, in 1991 by Iijima, due to its excellent electrical, thermal and mechanical proprieties. Its current-carrying capacity are up to 10^{10} A/cm^2, much greater than the capacity copper, which is less than 10^7 A/cm^2 [1],[5]. The mean free path of the CNT is larger than the copper's mean free path, allowing a ballistic transport beyond a great extension, which results in a lower resistivity [1]-[5]. Furthermore, the high thermal conductivity of the CNT is very important in its use as interconnects. These proprieties enable to a good electromigration reliability of the CNT, which is one of the major limitations on the performance of copper interconnects [1],[5],[6].

The CNT structure can be formed by a rolled-up graphene sheet, known as single-walled carbon nanotube (SWCNT), or by several concentric tubes forming a multilayer, called multi-walled carbon nanotube (MWCNT). The nanotube can be metallic or semiconductor, depending on the chiral angle and the chiral indexes of its structure [1],[2],[6]. Since MWCNTs have smaller mean free path than SWCNTs, they are less favorable for use in interconnects [1],[5]. However, the resistance of an isolated SWCNT can achieve high values. Thus, the arrangement of several SWCNTs in parallel is necessary, which is called a SWCNT bundle, so that it has a greater performance compared to copper interconnects [1],[3]. In this work, a comparison between SWCNT, SWCNT bundle and copper at different lengths is studied, analyzing their frequencies, attenuation and delay time. The 22 nm technology node was used. A similar comparison was done in [8], but now we are including copper interconnects, leading to a more accurate study.

II. SWCNT Interconnect Modeling

A. Resistance of CNT

The resistance of a SWCNT consists of three parts: the contact resistance between the metal and the nanotube (Rc), the quantum resistance (Rq) and the scattering resistance (Rs). The contact and quantum resistances are independent of CNT length. However, the scattering resistance depends on the length of the nanotube [1]-[5]. When the length of the SWCNT is less than its mean free path, which is typically 1

μm [1], the electron transport in the nanotube is essentially ballistic and the resistance does not depend on the length of the nanotube. If the length of the SWCNT is greater than the mean free path, there is the addition of the scattering resistance [1]-[3]. Equations (1) and (2) show the resistance of a CNT,

$$R_{CNT} = Rc + Rq; if : l_{CNT} \leq \lambda_{CNT} \quad (1)$$

$$R_{CNT} = Rc + Rq + Rs; if : l_{CNT} > \lambda_{CNT} \quad (2)$$

where l_{CNT} is the length of the CNT. The contact resistance can achieve the value of 100 kΩ [1],[3]. However, CNT with diameter around 1 nm has contact resistance in the order of few kilo ohms or even hundreds of ohms, indicating that it can be neglected when compared to the quantum resistance [4]. In this work, the contact resistance was considered to be perfect, i.e., Rc = 0. The quantum and scattering resistance are given in (3) and (4).

$$Rq = \frac{h}{4e^2} = 6{,}45k\Omega \quad (3)$$

$$Rs = \frac{h}{4e^2}\left(\frac{l_{CNT}}{\lambda_{CNT}}\right) \quad (4)$$

where e is the electron charge and h is the Planck's constant. The quantum resistance is equally divided into each side of the metal-nanotube contact [1]-[4].

B. Inductance of CNT

The motion of electrons carried by a conductor is modeled by the inductance, which consists of the magnetic and kinetic inductance [1]-[4]. The magnetic inductance is calculated considering that the CNT is a very thin wire, with diameter d, and positioned at a distance y from the ground plane. The magnetic inductance is calculated by (5). The kinetic inductance is given by the kinetic energy stored in each conducting channel of the CNT for an effective inductance. Equation (6) calculates the kinetic inductance.

$$L_M = \frac{\mu}{2\pi}\ln\left(\frac{y}{d}\right) \quad (5)$$

$$L_K = \frac{h}{2e^2 v_F} \quad (6)$$

where v_F is the Fermi's velocity, which is $8x10^5$ m/s for the CNT. Considering $d = 1nm$ e $y = 1\mu m$, L_M is 1.4pH/μm [2],[3]. The kinetic inductance value is 16nH/μm [1]-[4]. Since each CNT has four conducting channel in parallel that do not interact, the effective kinetic inductance is $L_K/4$ [1]-[3]. A good approximation of the total inductance L_{CNT} is 4nH/μm [3].

C. Capacitance of CNT

The capacitance of a SWCNT is formed by two parts, an electrostatic and a quantum capacitance [1]-[5]. The electrostatic and quantum capacitance are given, respectively, by (7) and (8).

$$C_E = \frac{2\pi\varepsilon}{\ln\left(\frac{y}{d}\right)} \quad (7)$$

$$C_Q = \frac{2e^2}{hv_F} \quad (8)$$

The electrostatic capacitance is influenced by the surrounding environment, regarding neighbors and ground planes of the CNT. Considering $d = 1\ nm$ and $y = 1\ \mu m$, C_E is 30aF/μm. The quantum capacitance refers to the influence of the quantum energy stored in the nanotube when it carries current. The value of the quantum capacitance is 100 aF/μm [1],[2]. Considering the four conducting channels described previously, the total capacitance of the CNT is given by (9).

$$C_{CNT} = \frac{C_E \cdot 4C_Q}{C_E + 4C_Q} \quad (9)$$

Hence, the equivalent circuit model for an isolated SWCNT is shown in Fig. 1.

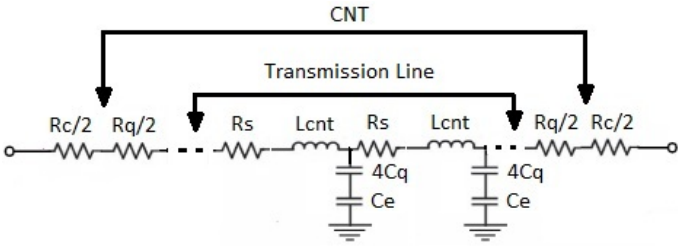

Fig. 1 Interconnect model of an isolated SWCNT

III. SWCNT Bundle Interconnect Modeling

The SWCNT bundle has a lower resistance than the isolated SWCNT, which is necessary to achieve comparable performances to copper interconnects [1],[2]. SWCNT bundle interconnects are formed by several SWCNTs packed in parallel. It is assumed that all SWCNTs are identical, metallic and that each one has the same potential [5]. Considering d as the diameter of the nanotube and x is the distance between the centers of two adjacent nanotubes, the SWCNT bundle can be densely packed, if $x = d$, or sparsely packed, if $x > d$. It is known that there is a separation between each nanotube due to Van der Waal's gap, which is at least 0.32 nm [1]. Therefore, the number of carbon nanotubes n_{CNT} available can be calculated by (10) and (11) [1]-[3].

$$n_{CNT} = \begin{Bmatrix} n_W n_H - \frac{n_H}{2}; if : n_H even \\ n_W n_H - \frac{n_H - 1}{2}; if : n_H odd \end{Bmatrix} \quad (10)$$

$$n_W = \left[\frac{w-d}{x}\right]; n_H = \left[\frac{h-d}{\left(\sqrt{3}/2\right)x}\right] + 1 \quad (11)$$

where w is the width and h is the height of the SWCNT bundle interconnect. Thus, n_W and n_H are the number of CNTs along the width and the height, respectively [1]-[3]. At the 22 nm technology node, considering SWCNT bundle dimensions of 22 nm width and 44 nm height [1],[5] and considering the separation between each nanotube due to Van der Waal's gap, the amount of SWCNTs can be calculated and is approximately 600.

The resistance and inductance of the SWCNT bundle, with n_{CNT} SWCNTs, are calculated by (12) and (13).

$$R_{bundle} = \frac{R_{CNT}}{n_{CNT}} \tag{12}$$

$$L_{bundle} = \frac{L_{CNT}}{n_{CNT}} \tag{13}$$

Considering that all SWCNTs are in the same potential, since all contacts between CNTs in the bundle are identical and that each SWCNT has the same mean free path (1), it is possible to assume that the interaction between adjacent CNTs in a SWCNT bundle is weak, and they carry currents independent of each other [1]-[5].

The SWCNT bundle capacitance is obtained by the combination of the quantum capacitance of all SWCNTs in parallel, called the quantum capacitance bundle C_Q^{bundle}, which is in series with the SWCNT bundle electrostatic capacitance C_E^{bundle} [1],[2]. The quantum capacitance is calculated by (14). Since the quantum capacitance is in series with the electrostatic capacitance, the total capacitance of the SWCNT bundle is obtained by (15).

$$C_Q^{bundle} = C_Q^{CNT} \cdot n_{CNT} \tag{14}$$

$$C_{bundle} = \frac{C_E^{bundle} \cdot C_Q^{bundle}}{C_E^{bundle} + C_Q^{bundle}} \tag{15}$$

The C_Q^{bundle} can be neglected for large values of n_{CNT}, and the value of the SWCNT bundle capacitance is approximately equal to its electrostatic capacitance [1],[4],[5],[6]. Srivastava et. al. [1] shows that the nanotubes inside the bundle are electrostatically shielded from the ground planes, and can be neglected. The edge nanotubes are the main contributors to the electrostatic capacitance of the SWCNT bundle. For 22 nm technology node, the capacitance of the SWCNT bundle is approximately 135aF/μm [1].

IV. Copper Interconnect Modeling

A. Resistance of Copper

The resistance of copper can be calculated using the following equation,

$$R_{Cu} = \frac{\rho \cdot l}{w \cdot t} \tag{16}$$

where l is the length of the copper, w is its width, t is its thickness and ρ is its resistivity. The resistivity of the copper , in nanometer scale, is formed by the combination of the superficial scattering and boundary scattering [3],[4],[9],[10]. These phenomena correspond to the parameters ρ_{FS} and ρ_{MS}, proposed by Fuchs and Sondheimer (ρ_{FS}) and by Mayadas e Shatzkes (ρ_{MS}) [3],[4]. Therefore, the resistivity of the copper, in nanometer scale, is calculated by (17).

$$R_{Cu} = \frac{\left(\rho_{FS} + \rho_{MS}\right) \cdot l}{w \cdot t} \tag{17}$$

According to [2],[11], the value of the resistivity of copper in the 22 nm technology for local interconnects is 4,666 μΩ-cm. However, the value of the copper's resistivity gets to 5,8 μΩ-cm for minimum values of the wire width [3],[4],[9]-[13]. In this work the value of 5,8 μΩ-cm for resistivity will be used in the 22 nm technology, that meets the requirements of ITRS [7].

B. Inductance of Copper

The self-inductance L and the mutual inductance M of the copper interconnection in nanometer scale is obtained using (18) and (19),

$$L = \frac{\mu_O \cdot l}{2\pi}\left[\ln\left(\frac{2l}{w+t}\right) + \frac{1}{2} + \frac{0.22(w+t)}{l}\right] \tag{18}$$

$$M = \frac{\mu_O \cdot l}{2\pi}\left[\ln\left(\frac{2l}{s}\right) - 1 + \frac{s}{l}\right] \tag{19}$$

where h is the height of the wire above the plan connected to earth, μ_o is the permeability and s is the space between the wires [2]-[4]. The total inductance of the copper L_{Cu} is given by the sum of the self and mutual inductance.

C. Capacitance of Copper

The capacitance of the copper interconnection is calculated by the sum of the coupling between two adjacent wires C_C and the capacitance connected to the ground plan C_g [2]-[4]. These capacitances can be obtained by (20) and (21) [3],

$$C_g = \varepsilon \cdot \left(\frac{w}{h} + 2.22\left(\frac{s}{s+0.7h}\right)^{3.19} + 1.17\left(\frac{s}{s+1.51h}\right)^{0.76} \cdot \left(\frac{t}{t+4.53h}\right)^{0.12} \right) \tag{20}$$

$$C_C = \varepsilon \cdot \left(1.14\frac{t}{s}\left(\frac{h}{h+2.06s}\right)^{0.09} + 0.74\left(\frac{w}{w+1.59s}\right)^{1.14} + 1.16\left(\frac{w}{w+1.87s}\right)^{0.16} \cdot \left(\frac{h}{h+0.98s}\right)^{1.18} \right) \tag{21}$$

where ε is the relative permissiveness for a dielectric constant. Considering (20) and (21) and according to [1],[7], for a dielectric constant equal to 2, the value of the capacitance of the copper C_{Cu} is approximately 150aF/μm, which will be used in this work.

The models in L, in π and in T are used as interconnects models for coppers [9]. Since the model in π is frequently used as distributed line [2],[4], it will be used in this work. Fig. 2 shows the interconnect model of copper [9].

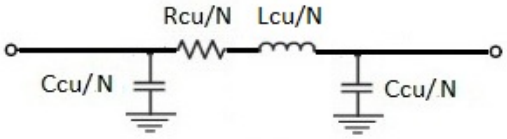

Fig. 2 Interconnect model of a copper

The precision of the model is determined by the number of segments 'N' that it has. A chain with more than three segments in π provides an error less than 3% [4]. In this work, three segments in π will be used.

V. Results and Analysis

A. Local Interconnections

Considering the simulation of each interconnection using the circuit of Fig. 3, the frequency in -3dB (f_{-3dB}) was obtained using local interconnections ($l_{CNT} \leq \lambda_{CNT}$), in other words, its passing band, verifying the maximum velocity that each interconnection supports.

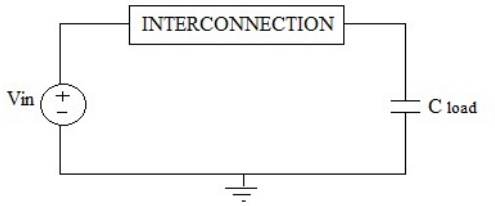

Fig. 3 Simulated circuit for each interconnection

Fig. 4 illustrates the behavior of the frequency of local interconnects, for different lengths. It is verified that, as the length of the interconnect increases, the frequency lowers. This occurs since the values of resistance, inductance and capacitance increases. These parameters are decisive in the out signal, being the signal more distorted as these values increases. It is noted that the SWCNT bundle and the copper have greater bandwidth than the isolated SWCNT, for any length. Besides that, the SWCNT bundle only has comparable bandwidth to copper for length above 700 nm.

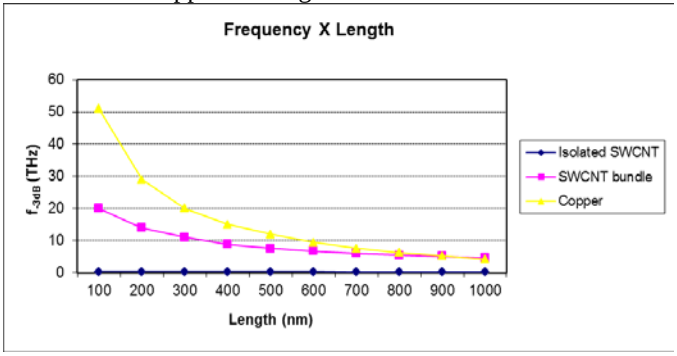

Fig. 4 Frequency versus length for local interconnects

The local interconnects of 10nm, 100nm and 1μm of length were minutely analyzed. Table I shows the frequency in -3dB of each material, for the analyzed lengths.

Table I Frequency in -3dB of each material, for $l_{CNT} \leq \lambda_{CNT}$

Local	Length (L)	Material	f_{-3dB}
Interconnection			
$l_{CNT} \leq \lambda_{CNT}$	10nm	Isolated SWCNT	253 GHz
		SWCNT bundle	66 THz
		Copper	232 THz
	100nm	Isolated SWCNT	300 GHz
		SWCNT bundle	20 THz
		Copper	51 THz
	1μm	Isolated SWCNT	230 GHz
		SWCNT bundle	4.7 THz
		Copper	4.2 THz

Therefore, it was chosen the same frequency, below the cutoff frequency of the three materials, to analyze and compare the attenuation (A) and the time delay in propagation (t_d) of the three lengths. In this way, it is possible to show the behavior of the signal in the bandwidth. Table II shows the comparative study between the isolated SWCNT, SWCNT bundle and copper, for the frequency of 200 GHz.

Table II Study of the interconnects with length in the range of $l_{CNT} \leq \lambda_{CNT}$

Freq.	L	Material	A(dB)	t_d(ps)
200GHz	10nm	Isolated SWCNT	-2.10	0.46
		SWCNT bundle	0.01	0.00
		Copper	0.00	0.00
	100nm	Isolated SWCNT	-1.55	0.51
		SWCNT bundle	0.01	0.00
		Copper	0.01	0.00
	1μm	Isolated SWCNT	-0.39	1.07
		SWCNT bundle	0.06	0.01
		Copper	0.00	0.07

From the analysis of Table II, it is possible to observe, at the frequency of 200 GHz, the attenuation of the signal and the delay of the isolated SWCNT. In this frequency, the delay of the isolated SWCNT is significant comparing to the period of the signal, that is 5ps, since the lower delay (for $l = 10nm$) is approximately 10% of the input signal period. However, for this same frequency, it is observed that the attenuation and the delay of SWCNT bundle and of copper are insignificant. This indicates that both materials have better performance, being more favorable to be used in local interconnects.

Thus, to better analyze the attenuation and the delay time of SWCNT bundle and of copper, the same procedure was done, comparing only both materials, for the frequency of 1THz. Table III shows this comparative study between SWCNT bundle and copper.

Table III Study of SWCNT bundle and copper interconnections with length in the range of $l_{CNT} \leq \lambda_{CNT}$

Freq.	L	Material	A(dB)	t_d(fs)
1THz	10nm	SWCNT bundle	0.01	1.13
		Copper	0.00	0.22
	100nm	SWCNT bundle	0.06	1.36
		Copper	0.01	2.40
	1µm	SWCNT bundle	1.45	6.47
		Copper	-0.13	56.23

Analyzing Table III, it is possible to observe that, at a frequency of 1 THz, the attenuation and the delay of the signal increases as the length of the interconnects increases. Considering the length of 100 nm, the delay time of the copper interconnection is bigger than SWCNT bundle delay time, which the greatest delay value (for $l = 1\mu m$) doesn't achieve 1% of the period of the input signal (1ps). This shows that, even though the bandwidth of the copper is bigger, the delay of SWCNT bundle is smaller. Thus, for local interconnections, the SWCNT bundle has comparable performance to that of copper [1].

Regarding attenuation, it is verified that, for some lengths, this has positive values. This occurs mainly when there is a peak on the graph of the frequency before it starts to decline. This peak is because of the resonant effect caused by the inductance, when this one has comparable values to the resistance and to the capacitance of the interconnection [14]. Therefore, this resonant effect was observed only in local interconnections of SWCNT bundle and of copper. Fig. 5 shows the magnitude versus frequency plots of the isolated SWCNT, SWCNT bundle and copper for 100nm length. It is possible to observe the resonant effect in both the SWCNT bundle and the copper plots.

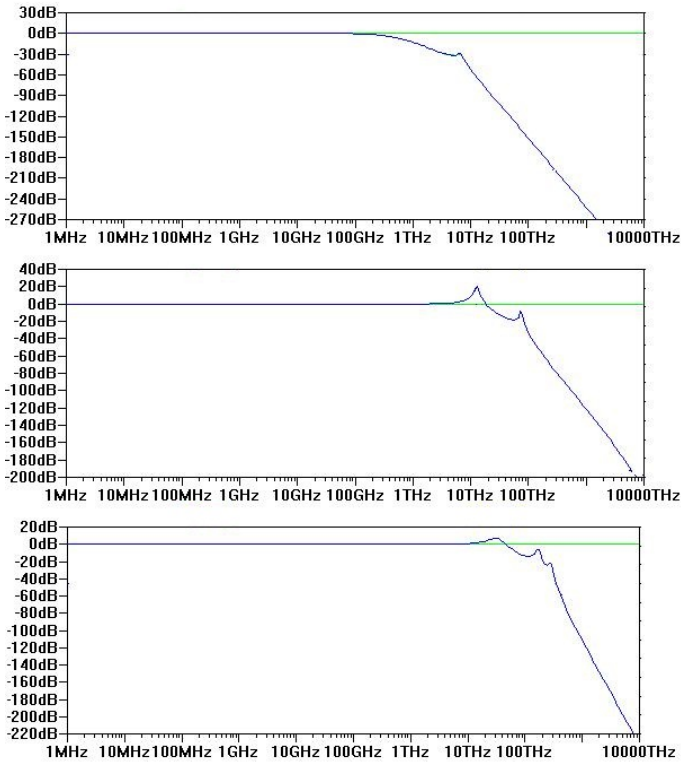

Fig. 5 Magnitude versus frequency plots for the isolated SWCNT (upper), the SWCNT bundle (middle) and the copper (under) with 100nm length

B. *Intermediate Interconnections*

Similar to the local interconnects, the frequency in -3dB of the intermediate interconnects ($l_{CNT} > \lambda_{CNT}$) were obtained, to see which maximum velocity the interconnect supports. Fig. 6 illustrates the behavior of the frequency of intermediate interconnects, considering different lengths.

As local interconnects, as the length of the interconnect increases, the frequency decreases. Besides that, the SWCNT bundle and the copper have better performance than the isolated SWCNT, considering any length. However, for intermediate interconnects, the SWCNT bundle has bigger bandwidth than the copper, for any length.

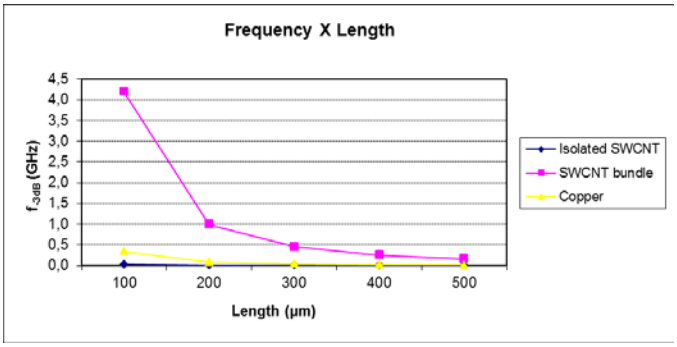

Fig. 6 Frequency versus length of intermediate interconnects

The intermediate interconnects of 10µm, 100µm and 500µm of length were minutely analyzed. Table IV shows the frequency in -3dB of each material, for different lengths.

Table IV Frequency in -3dB of each material, for $l_{CNT} > \lambda_{CNT}$

Intermediate Interconnect	Length (L)	Material	f_{-3dB}
$l_{CNT} > \lambda_{CNT}$	10µm	Isolated SWCNT	2.6 GHz
		SWCNT bundle	527 GHz
		Copper	34 GHz
	100µm	Isolated SWCNT	32 MHz
		SWCNT bundle	4.2 GHz
		Copper	345 MHz
	500µm	Isolated SWCNT	1.3 MHz
		SWCNT bundle	165 MHz
		Copper	14 MHz

The frequency of 1MHz was chosen, since it is below the cutoff frequency of three materials, so that the attenuation *A* and the delay time of propagation t_d are compared and analyzed considering the three lengths. Table V shows the comparative study between the isolated SWCNT, SWCNT bundle and copper.

Table V Study of the interconnects with lengths in the range of $l_{CNT} > \lambda_{CNT}$

Freq.	L	Material	A(dB)	t_d(ns)
1MHz	10µm	Isolated SWCNT	-0.02	0.08
		SWCNT bundle	0.00	0.00
		Copper	0.00	0.00
	100µm	Isolated SWCNT	-0.03	5.59
		SWCNT bundle	-0.01	0.05
		Copper	-0.04	0.56
	500µm	Isolated SWCNT	-1.98	102.17
		SWCNT bundle	0.00	1.10
		Copper	-0.03	13.01

Considering Table V, it is possible to observe that the attenuation and the delay time of the isolated SWCNT increases when the length of the interconnect increases. In this frequency, the delay in propagation of the isolated SWCNT is significant related to the period of the input signal, that is 1µs, being more than 10% of this period for a 500µm length. It is also possible to notice the increase in the delay time of the copper interconnect, being 1.3% of the period of the input signal for the length of 500µm.

For better analyzing the attenuation and time delay of SWCNT bundle and copper, the same procedure was followed, comparing only these two materials, for the frequency of 10MHz. Table VI shows the comparative study between SWCNT bundle and copper.

Table VI Study of SWCNT bundle and copper interconnects with length in the range of $l_{CNT} > \lambda_{CNT}$

Freq.	L	Material	A(dB)	t_d(ns)
10MHz	10µm	SWCNT bundle	0.00	0.00
		Copper	0.00	0.00
	100µm	SWCNT bundle	-0.01	0.05
		Copper	-0.04	0.54
	500µm	SWCNT bundle	-0.04	1.07
		Copper	-1.85	10.24

Analyzing Table VI, it is observed that, as the length of interconnects increases, the attenuation and the delay time of the copper interconnect signal are significant. The propagation delay of the copper interconnects, for $l = 500\mu m$, gets to 10% of the period of the input signal (100ns). On the other hand, the SWCNT bundle presents insignificant values of attenuation and delay in propagation. Therefore, for intermediate interconnections, the SWCNT bundle has better performance than the copper interconnect.

VI. Conclusions and Future Prospects

In this work, a comparative study between isolated SWCNT, SWCNT bundle and copper interconnects with different lengths was performed. The SWCNT bundle interconnects have better performance if compared to isolated SWCNT interconnects. In addition, the SWCNT bundle interconnects present better performance than copper interconnects considering attenuation and delay time. It was also observed that the SWCNT bundle can be used in circuits with very high frequencies, above tera Hertz, without distorting the input signal. In addition, the SWCNT bundle interconnects present better performance than copper interconnects considering attenuation and delay time. The smaller the interconnection length, the better the circuit performance. Therefore, SWCNT bundle interconnects are promising in the use in GSI and TSI integrated circuits.

For future prospects, these interconnects should also be analyzed in GSI and even TSI integrated circuits, such as nanoelectronic circuits.

Acknowledgment

The authors are grateful to CAPES, PQ/CNPq and INCT-NAMITEC for support.

References

[1] N. Srivastava, H. Li, F. Kreupl, K. Banerjee, (2009). "On the Applicability of Single-Walled Carbon Nanotubes as VLSI Interconnects", In: *IEEE Transactions on Nanotechnology*, vol. 8, no. 4, pp. 542-558.

[2] C. Thiruvenkatesan, J. Raja, (2009). "Studies on the Application of Carbon Nanotube as Interconnects for Nanometric VLSI Circuits", In: *ICETET'09*, pp. 162-167.

[3] D. Das, H. Rahaman, (2010). "Timing Analysis in Carbon Nanotube Interconnects with Process, Temperature, and Voltage Variations", In: *2010 International Symposium on Electronic System Design*, pp. 27-32.

[4] K-H. Koo, K.C.Saraswat, (2011), "Study of Performances of Low-k Cu, CNTs, and Optical Interconnects", In: Nanoelectronic Circuit Design, pp. 377-407.

[5] A. Srivastava, Y. Xu, A. K. Sharma, (2010). "Carbon nanotubes for next generation very large scale integration interconnects", In: *Journal of Nanophotonics*, vol. 4, no. 041690, pp. 1-26.

[6] A. Naeemi, J. D. Meindl, (2007). "Design and Performance Modeling for Single-Walled Carbon Nanotubes as Local, Semiglobal, and Global

Interconnects in Gigascale Integrated Systems", In: *IEEE Transactions on Electron Devices*, vol. 54, no. 1, pp. 26-37.

[7] International Technology Roadmap for Semiconductors (ITRS): Technical Report. 2014 Edition. Available: http://www.itrs.net (2014).

[8] C. P. S. M. Nogueira, J. G. Guimarães (2012). "Analysis of SWCNT Interconnects for GSI and TSI Integrated Circuits", In: *Microelectronics Technology and Devices – SBMicro 2012*, vol. 49, no. 1, pp. 247-253.

[9] H. B. Bakoglu, (1990). "Circuits, interconnections, and packaging for VLSI", Addison-Wesley Publshing Company, EUA.

[10] A. Naeemi, J. D. Meindl, (2008). "Performance Modeling for Single- and Multiwall Carbon Nanotubes as Signal and Power Interconnects in Gigascale Systems", In: *IEEE Transactions on Electron Devices*, vol. 55, no. 10, pp. 2574-2582.

[11] H. Li, W-Y. Yin, J-F. Mao, (2006). "Modeling of Carbon Nanotube Interconnects and Comparative Analysis with Cu Interconnects", In: *Proceedings of Asia-Pacific Microwave Conference 2006*, pp. 1361-1364.

[12] M. K. Rai, S. Sarkar, (2011). "Carbon Nanotube as VLSI Interconnect", In: *Electronic Proprieties of Carbon Nanotube*, pp. 475-494.

[13] Y. Xu, A. Srivastava, (2010). "A model for carbon nanotube interconnects", In: *Int. J. Circ. Theor. Appl. 2010*, vol. 38, no. 6, pp. 559–575.

[14] J. Rosenfeld, E. G. Friedman, (2009). "Quasi-Resonant Interconnects: A Low Power, Low Latency Design Methodology", In: *IEEE Transactions on Very Large Scale Integration (VLSI) Systems*, vol. 17, no. 2, pp. 181-193.